JOC Article

Organocatalytic Asymmetric Direct Phosphonylation of α,β-Unsaturated Aldehydes: Mechanism, Scope, and Application in Synthesis

Eddy Maerten, Silvia Cabrera, Anne Kjærsgaard, and Karl Anker Jørgensen*

Danish National Research Foundation, Center for Catalysis, Department of Chemistry, Aarhus University, DK-8000 Aarhus C, Denmark

kaj@chem.au.dk

Received August 24, 2007

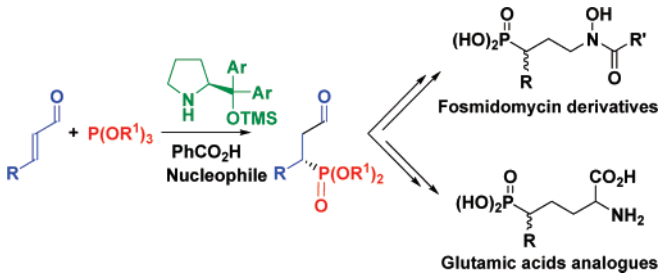

The first direct organocatalytic enantioselective phosphonylation of α,β-unsaturated aldehydes with phosphite, in combination with a Brønsted acid and a nucleophile, is presented. Mechanistic investigations have revealed that the first step in the catalytic process, after the formation of the iminium intermediate, is the addition of phosphite to the β-carbon atom, leading to the phosphonium ion−enamine intermediate. The rate-determining step for the reaction is the transformation of P(III) to P(V), which occurs via a nucleophilic S_N2-type dealkylation, and a screening of various nucleophiles shows that soft nucleophiles in combination with a Brønsted acid improve the reaction rate and enantioselectivity. The reaction conditions developed show that the use of 2-[bis(3,5-bistrifluoromethylphenyl)trimethylsilanoxymethyl]-pyrrolidine as the catalyst and tri-*iso*-propyl phosphite as the phosphonylation reagent, in the presence of stoichiometric amount of benzoic acid and sodium iodide, gave the β-phosphonylation of aromatic and aliphatic α,β-unsaturated aldehydes in good yields and enantioselectivities. The products formed by this new reaction have been used for the synthesis of a number of biologically important compounds, such as optically active hydroxyl phosphonate esters, phosphonic acids, and especially glutamic acid and fosmidomycin precursors, of which the two latter are showing important properties for the treatment of central nervous system diseases and as anti-malarial compounds, respectively. DFT calculations have been applied to explain the approach of the phosphite to the reactive carbon atom in the iminium intermediate in order to account for the observed absolute enantioselectivity in the reaction.

Introduction

Phosphonates and their phosphonic acid derivatives are widely used as chelating agents for bi- and trivalent metal ions. These binding abilities are even enhanced by the introduction of an amino group in the α-position to the phosphorus moieties. Compounds such as nitrilotris(methylenephosphonic acid) (NTMP), 1,2-diaminoethanetetrakis(methylenephosphonic acid) (EDTMP), and diethylenetriaminepentakis(methylenephosphonic acid) (DTPMP), the structure analogues to the well-known aminopolycarboxylates, nitrilotriacetic acid (NTA), ethylenediamine tetraacetic acid (EDTA), and diethylene triamine pentaacetic acid (DTPA), are described as stronger coordinating molecules.[1] The properties of these compounds have found important industrial applications, such as the use of phosphonates in desalination systems, in pulp and paper manufacturing, and in textile industry as peroxide bleach stabilizers. Another

(1) (a) Egli, T.; Bally, M.; Uetz, T. *Biodegradation* **1990**, *1*, 121. (b) Frey, S. T.; Horrocks, W. D., Jr. *Inorg. Chem.* **1991**, *30*, 1073. (c) Esser, S.; Wenclawiak, B. W.; Gabelmann, H. *Fresenius J. Anal. Chem.* **2000**, *368*, 250. (d) Schneppensieper, T.; Finkler, S.; Czap, A.; van Eldik, R.; Heus, M.; Nieuwenhuizen, P.; Wreesmann, C.; Abma, W. *Eur. J. Inorg. Chem.* **2001**, 491.

10.1021/jo7018587 CCC: $37.00
Published on Web 10/10/2007

SCHEME 1. Organocatalytic Enantioselective β-Phosphonylation of α,β-Unsaturated Aldehydes and the Synthesis of Fosmidomycin and Glutamic Acid Derivatives

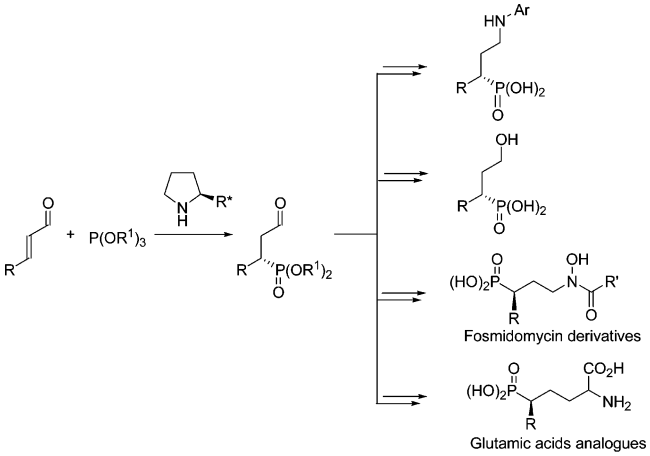

main application of these compounds in oil and gas industries is to inhibit scale formation.[2]

The phosphonates and their phosphonic acid derivatives can also be used in medicine to treat various bone and calcium metabolism diseases[3] and as carriers for radionuclides in bone cancer treatment (samarium-153 ethylenediamine tetramethylenephosphonate).[4] The α- and β-aminophosphonic acids also have important biological applications as they are known, by mimicking amino acids, to affect the physiological activity of the cell and to regulate important biological functions.[5] Further important applications are found for glutamic acid analogues and fosmidomycin derivatives. Glutamic acid analogues are used for the treatment of central nervous diseases such as epilepsy, Huntington's disease, Parkinson's disease, dementia, and chronic pain.[6] The substitution of the carboxylic acid group by a phosphonic acid moiety is known to increase receptor selectivity. The fosmidomycin derivatives have recently shown very promising biological activities in anti-malarial studies.[7]

Due to the biological properties of phosphonic acids and their derivatives, the development of specific and enantioselective pathways for oxo-phosphonylated compounds, which can easily provide a multitude of amino acid analogues, is of the great importance.

During the past decade, organocatalysis has become a powerful synthetic tool, affording, for example, efficient functionalization of aldehydes in an enantioselective manner.[8] By the application of organocatalysis, we will, in the following, describe a simple, general, enantioselective, and direct approach for the β-phosphonylation of α,β-unsaturated aldehydes,[9] the mechanistic development, the scope of the reaction, and the application of the optically active products obtained for the synthesis of precursors for glutamic acid analogues and fosmidomycin derivatives (Scheme 1). Furthermore, we will show that DFT calculations can explain the observed absolute configuration of the products obtained based on transition-state calculations.

Results and Discussion

Mechanistic Considerations. For the development of the enantioselective β-phosphonylation of α,β-unsaturated aldehydes, several considerations and challenges have to be taken into account. The proposed catalytic cycle is outlined in Figure 1.

The first step of the catalytic cycle consists in the iminium ion **5** formation from the condensation of the aldehyde **1** with catalyst **4**. The phosphite **2** then reacts with **5** to give the phosphonium ion−enamine intermediate **6**. The next step is proposed to involve a transformation of P(III) to P(V), which we consider can be performed via a nucleophilic substitution on the alkyl chain in the α-position to the oxygen atom of **6**, leading to the phosphonate−enamine intermediate **7**.[10] The

(2) (a) Gill, J. S.; Varsanik, R. G. *J. Cryst. Growth* **1986**, *76*, 57. (b) Duca, J. S.; Hopfinger, A. *J. Chem. Mater*. **2000**, *12*, 3821.

(3) Bones, calcium diseases, see: (a) Brown, D. L.; Robbins, R. *J. Clin. Pharmacol*. **1999**, *39*, 651. (b) Emkey, R.; Koltun, W.; Beusterien, K.; Seidman, L.; Kivitz, A.; Devas, V. *Curr. Med. Res. Opin*. **2005**, *21*, 1895. (c) Payer, J.; Killinger, Z.; Sulkova, I.; Celec, P. *Biomed. Pharmacother*. **2007**, *61*, 191.

(4) (a) Lewington, V. *J. Phys. Med. Biol.* **1996**, *41*, 2027. (b) Yang, Y. Q.; Luo, Sh. Zh.; Pu, M. F.; He, J. H.; Bing, W. Z.; Wang, G. Q. *J. Radioanal. Nucl. Chem.* **2003**, *1*, 133. (c) Maini, C. L.; Bergomi, S.; Romano, L.; Sciuto, R. *Eur. J. Nucl. Med. Mol. Imaging* **2004**, *1*, S171. (d) Olivier, P. *Nucl. Instrum. Methods A* **2004**, *527*, 4.

(5) (a) Kafarski, P.; Lejczak, B. *Phosphorus, Sulfur Silicon Relat. Elem*. **1991**, *62*, 193. For reviews, see: (b) Moonen, K.; Laureyn, I.; Stevens, C. V. *Chem. Rev*. **2004**, *104*, 6177. (c) Palacios, F.; Alonso, C.; de los Santos, J. M. *Chem. Rev*. **2005**, *105*, 899. (d) Ma, J.-A. *Chem. Soc. Rev*. **2006**, *35*, 630.

(6) (a) Moonen, K; Van Meenen, E.; Verwee, A.; Stevens, C. V. *Angew. Chem., Int. Ed.* **2005**, *44*, 7407. For review on glutamate receptors, see: (b) Bräuner-Osborne, H.; Egebjerg, J.; Nielsen, E. Ø.; Madsen, U.; Krogsgaard-Larsen, P. *J. Med. Chem.* **2000**, *43*, 2609. See also: (c) Tanabe, Y.; Nomura, A.; Masu, M.; Shigemoto, R.; Mizuno, N.; Nakanishi, S. *J. Neurosci.* **1993**, *13*, 1372. (d) Nakajima, Y.; Iwakabe, H.; Akazawa, C.; Nawa, H.; Shigemoto, R.; Mizuno, N.; Nakanishi, S. *J. Biol. Chem.* **1993**, *268*, 11868. (e) Okamoto, N.; Hori, S.; Akazawa, C.; Hayashi, Y.; Shigemoto, R.; Mizuno, N.; Nakanishi, S. *J. Biol. Chem.* **1994**, *269*, 1231.

(7) (a) Missinou, M. A.; Borrmann, S.; Schindler, A.; Issifou, S.; Adegnika, A. A.; Matsiegui, P. B.; Binder, R.; Lell, B.; Wiesner, J.; Baranek, T.; Jomaa, H.; Kremsner, P. G. *Lancet* **2002**, *360*, 1941. (b) Lell, B.; Ruangweerayut, R.; Wiesner, J.; Missinou, M. A.; Schindler, A.; Baranek, T.; Hintz, M.; Hutchinson, D.; Jomaa, H.; Kremsner, P. G. *Antimicrob. Agents Chemother*. **2003**, *47*, 735. (c) Kurz, T.; Schlüter, K.; Kaula, U.; Bergmann, B.; Walter, R. D.; Greffken, D. *Bioorg. Med. Chem.* **2006**, *14*, 5121. (d) Schlüter, K.; Walter, R. D.; Bergmann, B.; Kurz, T. *Eur. J. Med. Chem.* **2006**, *41*, 1385. (e) Haemers, T.; Wiesner, J.; Van Poecke, S.; Goeman, J.; Henschker, D.; Beck, E.; Jomaa, H.; Van Calenbergh, S. *Bioorg. Med. Chem. Lett.* **2006**, *16*, 1888. (f) Devreux, V.; Wiesner, J.; Jomaa, H.; Rozenski, J.; Van der Eycken, J.; Van Calenbergh, S. *J. Org. Chem.* **2007**, *72*, 3783.

(8) For recent reviews on organocatalysis, see: (a) Dalko, P. I.; Moisan, L. *Angew. Chem., Int. Ed.* **2004**, *43*, 5138. (b) Berkessel, A.; Gröger, H. *Asymmetric Organocatalysis*; VCH: Weinheim, Germany, 2004. (c) *Acc. Chem. Res.* **2004**, *37* (8), special issue on organocatalysis. (d) Seayed, J.; List, B. *Org. Biomol. Chem.* **2005**, *3*, 719. (e) List, B. *Chem. Commun.* **2006**, 819. (f) Lelais, G.; MacMillan, D. W. C. *Aldrichimica Acta* **2006**, *39*, 79. (g) Gaunt, M. J.; Johansson, C. C. C.; McNally, A.; Vo, N. C. *Drug Discovery Today* **2007**, *2*, 8. (h) Dalko, P. I., Ed. *Enantioselective Organocatalysis*; Wiley-VCH: Weinheim, Germany, 2007. For a review on α-functionalization, see: (i) Marigo, M.; Jørgensen, K. A. *Chem. Commun.* **2006**, 2001. (j) Guillena, G.; Ramón, D. J. *Tetrahedron: Asymmetry* **2006**, *17*, 1465. For a review on β-functionalization, see: (k) Svetlana, B. Tsogoeva S. V. *Eur. J. Org. Chem.* **2007**, *11*, 1701. (l) Almaşi, D.; Alonso, D. A.; Nájera, C. *Tetrahedron: Asymmetry* **2007**, *18*, 299. For a selected exemple of γ-functionalization, see: (m) Bertelsen, S.; Marigo, M.; Brandes, S.; Dinér, P.; Jørgensen, K. A. *J. Am. Chem. Soc.* **2006**, *128*, 12973. For review on organocatalytic multicomponent reactions, see: (n) Enders, D.; Grondal, C.; Hüttl, M. R. M. *Angew. Chem., Int. Ed.* **2007**, *46*, 1570. (o) Guillena, G.; Ramón, D. J.; Yus, M. *Tetrahedron: Asymmetry* **2007**, *18*, 693.

(9) (a) Enders, D.; Saint-Dizier, A.; Lannou, M. I.; Lenzen, A. *Eur. J. Org. Chem*. **2006**, 29. For organocatalytic hydrophosphination, see: (b) Carlone, A.; Bartoli, G.; Bosco, M.; Sambri, L.; Melchiorre, P. *Angew. Chem., Int. Ed.* **2007**, *46*, 4504. (c) Ibrahem, I.; Rios, R.; Vesely, J.; Hammar, P.; Eriksson, L.; Himo, F.; Córdova, A. *Angew. Chem., Int. Ed.* **2007**, *46*, 4507. Recently an approach for β-nitrophosphates has been published: (d) Wang, J.; Heikkinen, L. D.; Li, H.; Zu, L.; Jiang, W.; Xie, H.; Wang, W. *Adv. Synth. Catal*. **2007**, *349*, 1052.

(10) Bhattacharya, A. K.; Thyagarajan, G. *Chem. Rev.* **1981**, *81*, 415.

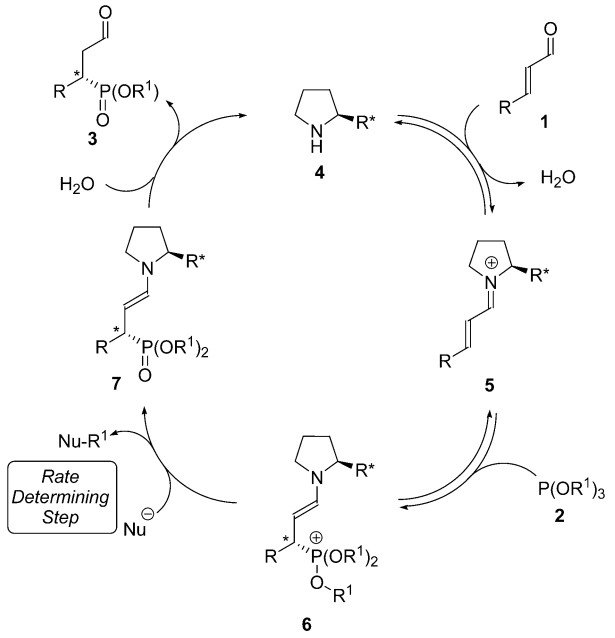

FIGURE 1. Proposed catalytic cycle.

overall result of these two steps is the conversion of trivalent phosphorus into pentavalent phosphorus. Hydrolysis of **7** regenerates the catalyst and liberates the optically active phosphonate **3**. One of the challenges in the catalytic cycle is the P(III) to P(V) transformation in order to obtain a catalytic cycle. Thus, in addition to the optimization for the *β*-functionalization of α,*β*-unsaturated aldehydes, an extra nucleophile, necessary for a S_N2-type dealkylation reaction of one of the phosphorus alkoxy groups, affording the phosphonate without competing with the desired 1,4-conjugate addition, has to be considered.

A further challenge in the development of the enantioselective *β*-phosphonylation of α,*β*-unsaturated aldehydes is to control the chemoselectivity, as both an 1,4- and 1,2-addition reaction can take place as outlined in Scheme 2. The phosphite addition, catalyzed by a secondary amine, proceeds via an iminium ion formation, known to lower the LUMO of the α,*β*-unsaturated

TABLE 1. Screening of Reaction Conditions for Addition of $P(OMe)_3$ 2a to 2-Hexenal 1a[a]

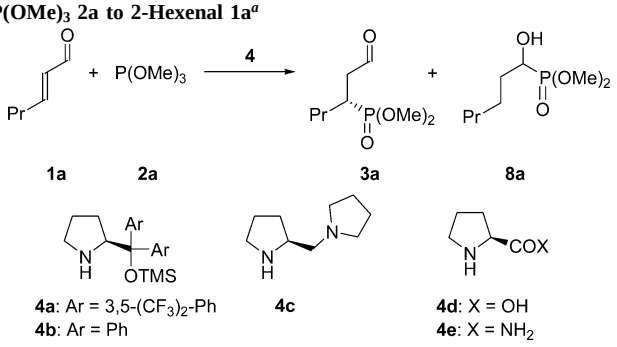

entry	solvent	cat.	conv.[b,c] (%)	ratio[b] **3a**/**8a**	ee[d] (%)
1	toluene	**4a**	70 (35)	80:20	n.d.
2	$CHCl_3$	**4a**	80	75:25	–
3	H_2O	**4a**	90	40:60	–
4	MeOH	**4a**	100 (54)[e]	100:0	n.d.
5	CH_2Cl_2	**4a**	100 (62)	100:0	50
6	CH_2Cl_2	**4b**	100 (60)	100:0	25
7	CH_2Cl_2	**4c**	100 (58)	100:0	12
8	CH_2Cl_2	**4d**	100 (53)	100:0	0
9	CH_2Cl_2	**4e**	70	67:33	n.d.

[a] Reactions were performed in 24 h between **1a** (0.9 mmol, 3 equiv), **2a** (0.3 mmol, 1 equiv) in presence of 10 mol % of the indicated catalyst **4**, and 2 equiv of $PhCO_2H$ in 3 mL of solvent. [b] Estimated by ^{31}P NMR. [c] The value in parentheses corresponds to the yield of product **3**. [d] Determined by HPLC after reductive amination of the aldehydes with aniline (see Supporting Information). [e] MeOH addition was observed as a byproduct.

SCHEME 2. The 1,4- and 1,2-Chemoselectivity

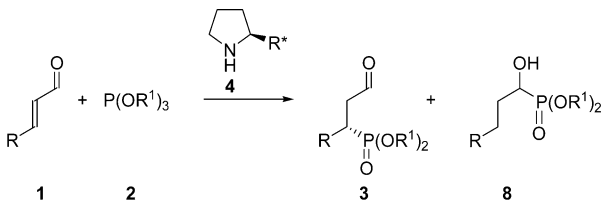

system, leading to a better chemoselectivity toward the 1,4-Michael addition type product.

In an attempt to overcome these requirements and challenges, the 2-[bis(3,5-bistrifluoromethylphenyl)trimethylsilanoxymethyl]pyrrolidine, catalyst **4a**, which has shown to be a general and convenient catalyst for aldehyde functionalizations,[11] was chosen to start our investigations. To our delight, 2-hexenal **1a** reacted with trimethyl phosphite **2a** in toluene in the presence of a catalytic amount of **4a** and a stoichiometric amount of $PhCO_2H$ to afford **3a** and **8a**, corresponding to the 1,4- and 1,2-phosphite addition adducts, respectively, in a 4:1 ratio (Table 1, entry 1). We examined several other solvents in order to control the chemoselectivity of the reaction; it was found that the reaction proceeds with lower ratio of **3a**/**8a** when H_2O or $CHCl_3$ was used (entries 2 and 3). Interestingly, the reaction was completely chemoselective in favor of the desired product **3a** in MeOH, but unfortunately, byproducts corresponding to the solvent addition were also observed giving a complex reaction mixture (entry 4). Finally, we found that CH_2Cl_2 was the solvent of choice, as **3a** was obtained as a single product in 62% yield and 50% ee (entry 5).

The screening of other secondary amines showed that catalysts **4b** and **4c** were also suitable for the reaction; however, lower enantiomeric excess of **3a** was obtained (Table 1, entries

(11) For recent applications of the use of protected diarylprolinols in catalysis, see: (a) Marigo, M.; Wabnitz, T. C.; Fielenbach, D.; Jørgensen, K. A. *Angew. Chem., Int. Ed.* **2005**, *44*, 794. (b) Marigo, M.; Fielenbach, D.; Braunton, A.; Kjærsgaard, A.; Jørgensen, K. A. *Angew. Chem., Int. Ed.* **2005**, *44*, 3703. (c) Franzén, J.; Marigo, M.; Fielenbach, D.; Wabnitz, T. C.; Kjærsgaard, A.; Jørgensen, K. A. *J. Am. Chem. Soc.* **2005**, *127*, 18296. (d) Hayashi, Y.; Gotoh, H.; Hayashi, T.; Shoji, M. *Angew. Chem., Int. Ed.* **2005**, *44*, 4212. (e) Marigo, M.; Franzén, J.; Poulsen, T. B.; Zhuang, W.; Jørgensen, K. A. *J. Am. Chem. Soc.* **2005**, *127*, 6964. (f) Shi, Y.; Gellman, S. H. *Org. Lett.* **2005**, *7*, 4253. (g) Sunden, H.; Ibrahem, I.; Córdova, A. *Tetrahedron Lett.* **2006**, *47*, 99. (h) Carlone, A.; Marigo, M.; North, C.; Landa, A.; Jørgensen, K. A. *Chem. Commun.* **2006**, 4928. (i) Ibrahem, I.; Córdova, A. *Chem. Commun.* **2006**, 1760. (j) Hansen, H. M.; Longbottom, D. A.; Ley, S. V.; *Chem. Commun.* **2006**, 4838. (k) Bertelsen, S.; Dinér, P.; Johansen, R. L.; Jørgensen, K. A. *J. Am. Chem. Soc.* **2007**, *129*, 1536. (l) Vesely, J.; Ibrahem, I.; Zhao, G.-L.; Rios, R.; Córdova, A. *Angew. Chem., Int. Ed.* **2007**, *46*, 778. (m) Enders, D.; Huettl, M. R. M.; Runsink, J.; Raabe, G.; Wendt, B. *Angew. Chem., Int. Ed.* **2007**, *46*, 467. (n) Zu, L.; Li, H.; Xie, H.; Wang, J.; Jiang, W.; Tang, Y.; Wang, W. *Angew. Chem., Int. Ed.* **2007**, *46*, 3732. (o) Carlone, A.; Cabrera, S.; Marigo, M.; Jørgensen, K. A. *Angew. Chem., Int. Ed.* **2007**, *46*, 1101. (p) Rios, R.; Sunden, H.; Vesely, J.; Zhao, G.-L.; Dziedzic, P.; Córdova, A. *Adv. Synth. Catal.* **2007**, *349*, 1028. (q) Hayashi, Y.; Okano, T.; Aratake, S.; Hazelard, D. *Angew. Chem., Int. Ed.* **2007**, *46*, 4922. (r) Alemán, J.; Cabrera, S.; Maerten, E.; Overgaard, J.; Jørgensen K. A. *Angew. Chem., Int. Ed.* **2007**, *46*, 5520. For a review, see: (s) Palomo, C.; Mielgo, A. *Angew. Chem., Int. Ed.* **2006**, *45*, 7876.

SCHEME 3. Temperature and Phosphite Substitution Effect

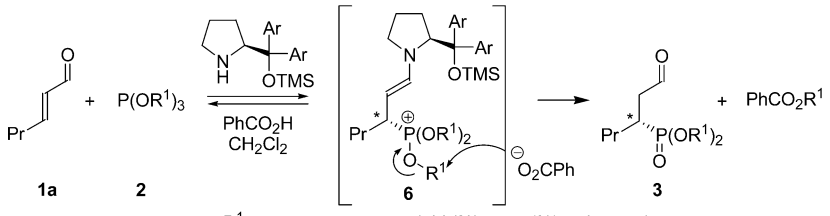

R^1	temp	time	yield (%)	ee (%)	by-product
2a: Me	rt	1 d	63	50	$PhCO_2Me$
2b: Et	rt	1 d	52	53	$PhCO_2Et$
2b: Et	-24°C	3 d	15	75	$PhCO_2Et$

6 and 7). L-Proline **4d** also catalyzed the β-phosphonylation; however, the obtained product was racemic (entry 8), whereas proline amide **4e** gave a mixture of **3a** and **8a** (entry 9).

We then considered modifying the reaction temperature and the steric hindrance induced by the phosphite used as nucleophile (Scheme 3).

The experiments showed that the enantioselectivity was only increased from 50 to 53% ee, changing trimethyl phosphite **2a** to triethyl phosphite **2b** at room temperature, while the use of **2b** at −24 °C improved the enantioselectivity to 75% ee as shown in Scheme 3. Unfortunately, at low temperature, the reaction also became extremely sluggish, leading to low yields even after long reaction time. However, these reactions permitted us to observe by ^{1}H NMR spectroscopy the progressive formation of $PhCO_2Me$ or $PhCO_2Et$ as byproducts using **2a** and **2b** as the phosphonylation reagents, respectively, during the reaction. These studies showed that the benzoate, as a nucleophile, plays an important role for the P(III)−P(V) transformation.

It was observed that the nucleophilic substitution reaction, the transformation from the phosphonium ion−enamine intermediate **6** to the phosphonate−enamine intermediate **7** in Figure 1, was the rate-determining step in the catalytic cycle. In order to try to increase the reaction rate and, hopefully, to improve also the enantioselectivity decreasing the temperature, the search for a more favorable nucleophile than benzoate was carried out. The Swain−Scott nucleophilicity parameters *n* were used for guidance. Some representative nucleophilicity parameters in relation to the nucleophiles used in the following are given in Table 2.

On the basis of the Swain−Scott parameters in Table 2, it should be expected that nucleophiles having a high *n* value would be able to increase the reaction rate in the catalytic cycle. Therefore, the role of thiophenol, NaI, phenol, and NaCl for the catalytic cycle of the reaction of 2-hexenal **1a** with different phosphites in CH_2Cl_2 was studied. When thiophenol is used as the nucleophile for the reaction of **1a** with triethyl phosphite **2b**, the only observed reaction consists of the well-documented thiol addition to the β-position (Table 3, entry 1).[13] The use of NaI or phenol could induce the desired 1,4-addition; however, the reactivity was low in both cases (entries 2 and 3), while no reaction was observed for NaCl (entry 4). Next, the combination of the benzoic acid and a nucleophile was studied. When phenol was used as the second additive, the conversion was still incomplete after 24 h, affording low yield of **3b** (entry 5), while NaI gave a tremendously enhanced reactivity and full conversion was obtained in less than 1 h (entry 6). Furthermore, to our surprise, the enantioselectivity of **3b** was also improved from 53 to 76% ee. It should be noted that with this catalytic system the enantioselectivity is independent of the temperature (entry 7). The countercation of the nucleophile additive also proved to be of importance, as shown by the reaction conducted in presence of KI and benzoic acid. It was found that the use of these reaction conditions also activated the carbonyl group of the corresponding β-phosphonylated 1,4-addition adduct **3b**, leading to a sequential 1,4−1,2-addition as the major reaction sequence (entry 8). It has also recently been observed for the hydrophosphination of α,β-unsaturated aldehydes that the effect of acid as cocatalyst can lead to important enantioselectivity variations.[9b] Next, electron-rich and electron-poor benzoic acid derivatives were tested, leading to identical enantioselectivity; however, for *p*-methoxy benzoic acid, a significantly lower reactivity was observed, compared to *p*-nitro benzoic acid (entries 10 and 11).

The steric hindrance of the phosphite is also important; for tri-*iso*-propyl phosphite **2c**, the reaction was slower, but an increase of both the yield (64%) and enantioselectivity (84% ee) was found (Table 3, entry 12). Finally, no β-phosphonylation reaction was observed with triphenyl phosphite **2d** as the nucleophilic substitution cannot occur on the aromatic fragment (entry 13), justifying our mechanistic proposal with the S_N2-type dealkylation reaction of one of the phosphorus alkoxy groups as of utmost importance for the catalytic cycle.

Our studies of the different reaction parameters led us to choose **4a** as the catalyst and tri-*iso*-propyl phosphite **2c** as the

TABLE 2. The Nucleophilicity Parameter *n* of Some Nucleophiles[12]

nucleophile	*n*
$C_6H_5S^-$	9.92
I^-	7.42
Br^-	5.79
$C_6H_5O^-$	5.75
C_6H_5SH	5.70
$C_6H_5CO_2^-$	4.50
Cl^-	4.37

(12) (a) Pearson, R. G.; Sobel, H.; Songstad, J. *J. Am. Chem. Soc.* **1968**, *90*, 319. (b) Swain, C. S.; Scott, C. B. *J. Am. Chem. Soc.* **1953**, *75*, 141. (c) Methot, J. L.; Roush, W. R. *Adv. Synth. Catal.* **2004**, *346*, 1035.

(13) (a) Hiemstra, H.; Wynberg, H. *J. Am. Chem. Soc.* **1981**, *103*, 417. (b) McDaid, P.; Chen, Y.-G.; Deng, L. *Angew. Chem., Int. Ed.* **2002**, *41*, 338. (c) Marigo, M.; Schulte, T.; Franzén, J.; Jørgensen, K. A. *J. Am. Chem. Soc.* **2005**, *127*, 15710. (d) Wang, W.; Li, H.; Wang, J.; Zu, L. *J. Am. Chem. Soc.* **2006**, *128*, 10354. (e) Brandau, S.; Maerten, E.; Jørgensen, K. A. *J. Am. Chem. Soc.* **2006**, *128*, 14986. (f) Rios, R.; Sundén, H.; Ibrahem, I.; Zhao, G.-L.; Eriksson, L.; Córdova, A. *Tetrahedron Lett.* **2006**, *47*, 8547. (g) Zu, L.; Wang, J.; Li, H.; Xie, H.; Jiang, W.; Wang, W. *J. Am. Chem. Soc.* **2007**, *129*, 1036. (h) Li, H.; Zu, L.; Xie, H.; Wang, J.; Jiang, W.; Wang, W. *Org. Lett.* **2007**, *9*, 1833. (i) Ishino, T.; Oriyama, T. *Chem. Lett.* **2007**, *36*, 550. For a review see: (j) Enders, D.; Luettgen, K.; Narine, A. A. *Synthesis* **2007**, *7*, 959.

TABLE 3. Optimization of Reaction Conditions: Nucleophiles, Benzoic Acids, and Phosphites[a]

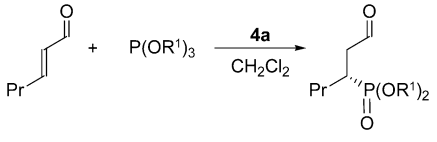

entry	time (h)	phosphite	additive[b]	temp	yield (%)	ee[c] (%)
1	24	**2b**	PhSH (2)	rt	**3b** − 0[d]	−
2	24	**2b**	NaI (2)	rt	**3b** − <5	n.d.
3	24	**2b**	PhOH (2)	rt	**3b** − <5	n.d.
4	24	**2b**	NaCl (2)	rt	**3b** −n.r	−
5	24	**2b**	PhOH (1)/$PhCO_2H$ (2)	rt	**3b** − 25[e]	40
6	1	**2b**	NaI (1)/$PhCO_2H$ (2)	rt	**3b** − 50	76
7	15	**2b**	NaI (1)/$PhCO_2H$ (2)	−24	**3b** − n.d.	76
8	2	**2b**	KI (1)/$PhCO_2H$ (2)	rt	**3b** − n.d.[f]	−
9	24	**2b**	LiI (1)/$PhCO_2H$ (2)	rt	**3b** − 48	76
10	1	**2b**	NaI (1)/4-NO_2-$PhCO_2H$ (2)	rt	**3b** − 47	76
11	24	**2b**	NaI (1)/4-MeO-$PhCO_2H$ (2)	rt	**3b** − 48	76
12	5	**2c**	NaI (1)/$PhCO_2H$ (2)	rt	**3c** − 61	84
13	24	**2d**	NaI (1)/$PhCO_2H$ (2)	rt	**3d** − n.r.	−

[a] Reactions were performed between **1a** (0.9 mmol, 3 equiv), **2** (0.3 mmol, 1 equiv) in the presence of 10 mol % of the catalyst **4a**, and the corresponding additives in 3 mL of CH_2Cl_2. [b] The numbers in parentheses correspond to the number of equivalents used. [c] Determined by HPLC after derivatization into the corresponding ester (see Scheme 4). [d] 1,4-Thiophenol addition was observed by NMR. [e] Incomplete reaction. [f] The 1,2- and 1,4−1,2-additions were also observed as the major products.

phosphonylation reagent, in the presence of stoichiometric amount of $PhCO_2H$ and NaI as additives in CH_2Cl_2. With these optimized conditions, the 1,4-addition of phosphites to α,β-unsaturated aldehydes occurs with a complete chemoselectivity and a good enantiocontrol.

Scope of the β-Phosphonylation Reaction. We then explored the scope of the reaction by reacting a number of different α,β-unsaturated aldehydes with tri-*iso*-propyl phosphite **2c** using the optimized reaction conditions developed above. The results are presented in Table 4.

The organocatalytic enantioselective β-phosphonylation reaction for the aliphatic α,β-unsaturated aldehydes proceeds with good yields and enantioselectivities (84−85% ee) (entries 1 and 3). The application of the enantiomeric catalyst (*R*)-**4a** for the phosphite addition of **2c** to **1a** afforded the enantiomeric product *ent*-**3c** in 55% yield with an enantioselectivity of 82% ee (entry 2). Similar enantiomeric excesses were obtained for the functionalized enals **1c** and **1d**; however, the yield was slightly lower (entries 4 and 5). To our delight, the reaction was also suitable for aromatic α,β-unsaturated aldehydes, such as cinnamic aldehyde **1e** and its *para*-substituted derivatives. For these aromatic α,β-unsaturated aldehydes, the corresponding phosphonates were obtained in 51−67% yield and 74−88% ee (entries 6−9). Finally, heteroaromatic α,β-unsaturated aldehydes, such as 2-furyl **1h** and 2-thiophene acrolein **1i**, can also be used for the phosphonylation process, and the optically active products were obtained in 74 and 84% ee, respectively (entries 10 and 11).

All of the compounds **3** are oils, and only a few of their corresponding alcohols **9** are solids. These solid alcohols can be enantiomerically enriched by recrystallization; for example, alcohol **9h** was obtained as enantiomerically pure (>99% ee) by recrystallization of a 88% ee sample in Et_2O at 4 °C.

Absolute Configuration and DFT Calculations of Transition States. For the Michael addition step, the organocatalyst

TABLE 4. Scope of the β-Phosphonylation of α,β-Unsaturated Aldehydes Catalyzed by 4a[a]

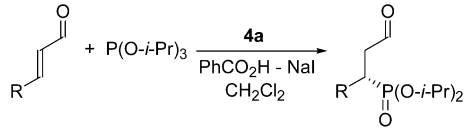

entry	R	cat.	yield (%)	ee[b] (%)
1	Pr, **1a**	(*S*)-**4a**	**3c** − 61	84
2	Pr, **1a**	(*R*)-**4a**	*ent*-**3c** − 55	−82
3	Et, **1b**	(*S*)-**4a**	**3e** − 54	85
4	(Z)-*n*-hex-3-en, **1c**	(*S*)-**4a**	**3f** − 46	84
5	$CH_2CH_2OTBDMS$, **1d**	(*S*)-**4a**	**3g** − 41	82
6	C_6H_5, **1e**	(*S*)-**4a**	**3h** − 51	83 (99)[c]
7	*p*-$MeOC_6H_4$, **1f**	(*S*)-**4a**	**3i** − 67	88
8	*p*-$NMe_2C_6H_4$, **1g**	(*S*)-**4a**	**3j** − 55	74
9	*p*-Cl−C_6H_4, **1j**	(*S*)-**4a**	**3k** − 59	88
10	2-furyl, **1h**	(*S*)-**4a**	**3l** − 60	74
11	2-thiophene, **1i**	(*S*)-**4a**	**3m** − 50	84

[a] Reactions were performed using α,β-unsaturated aldehydes **1** (0.9 mmol, 3 equiv), tri-*iso*-propyl phosphite **2c** (0.3 mmol, 1 equiv) in the presence of 10 mol % of catalyst **4a**, 2 equiv of $PhCO_2H$, and 1 equiv of NaI in 3 mL of CH_2Cl_2. [b] Determined by HPLC after derivatization into the corresponding alcohol or ester (see Scheme 4). [c] After recrystallization of the corresponding alcohol **9h**.

(*S*)-**4a** is effective for the iminium ion activation, and via sterical shielding of one of the faces of the α,β-unsaturated aldehyde, good enantiocontrol of the reaction is found. The absolute configuration of the product was assigned by a single-crystal X-ray analysis of **9h**, and the structure is shown Figure 2.[14]

The absolute configuration of **9h** indicates that in the chiral iminium ion intermediate **5** (see catalytic cycle in Figure 1) the

(14) X-ray crystal structure analysis of **9h**: formula $C_{15}H_{25}O_4P$, weight 300.32 g mol^{-1}. See Supporting Information.

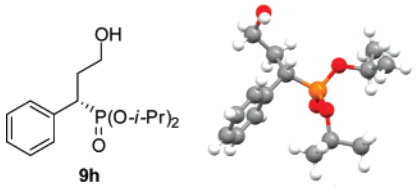

FIGURE 2. X-ray crystal structure of (*S*)-**9h**.

two aryl substituents and the OTMS group in the 2-position in the chiral pyrrolidine shield the "upper face", allowing the tri-*iso*-propyl phosphite **2c** to approach from "below" to the β-carbon atom. On the basis of this assumption, we have performed a series of DFT calculations[15] in order to understand the enantioselection in the reaction. The transition states for approach to the different faces of the reactive carbon atom in the chiral iminium ion **5** (see Figure 1) have been optimized at a B3LYP/6-31G(d) level of theory.[16] As the model reagent for the reaction, we have studied trimethyl phosphite **2a**, adding to the iminium ion generated from reaction of catalyst **4a** with 2-hexenal. Due to the complexity of the reaction course, we have not taken the role of NaI and benzoic acid into account for the enantioselective step, but will only focus on the addition of **2a** to the chiral iminium ion intermediate.

We have studied the approach of trimethyl phosphite **2a** to two different iminium ion intermediates, *anti* or *syn*, relative to the 2-substituent in the catalyst. For each iminium ion, the attack can occur from above or below, leading to four transition states. Of these transition states, three have been studied, and these are shown in Figure 3. The two first intermediates are **10**-*anti*-below and **10**-*syn*-below, in which the alkene fragment is *anti* or *syn*, relative to the 2-substituent in the catalyst. An approach of **2a** from below to these two intermediates will give opposite absolute configuration in the products, while an approach to the upper face in **10**-*anti*-upper will give the same absolute configuration of the product as the approach outlined in **10**-*syn*-below. We have excluded an approach of phosphate to the *syn*-intermediate to the upper face due to steric repulsion. The nucleophilic attack of **2a** in **10**-*anti*-below and **10**-*syn*-below corresponds to an approach to the less shielded face, while for **10**-*anti*-upper, the reaction will proceed to the most shielded face.

The calculated transition state shown in Figure 4, **TS-1**, corresponds to an attack of trimethyl phosphite **2a** to the nonshielded face of the (*E*)-iminium ion (**10**-*anti*-below), leading

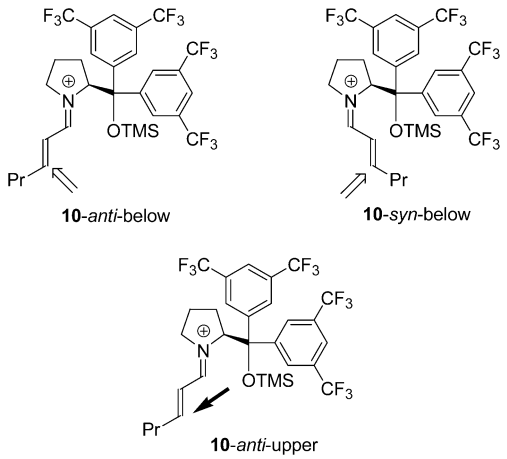

FIGURE 3. Intermediates used for the transition-state calculations.

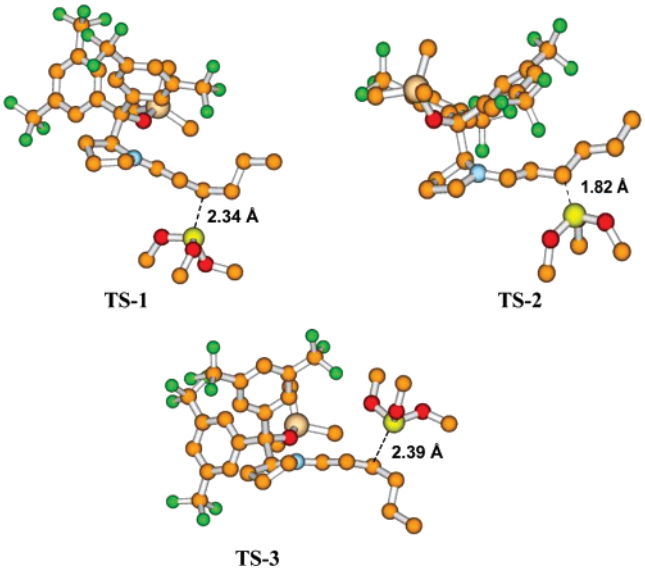

FIGURE 4. DFT-optimized transition-state structures for the three reaction paths leading to the *R*- (**TS-1**) and *S*-configuration (**TS-2** and **TS-3**) in the product, respectively. Calculated C−P distances [Å] are shown.

TABLE 5. Calculated Energies and C−P Bond Distances of the Three Transition States

	G (Hartree)	ΔG (kcal mol^{-1})	C−P[a] (Å)
TS-1	−3466.074669	0	2.34
TS-2	−3466.059994	9.2	1.82
TS-3	−3466.070676	2.5	2.39

[a] Calculated C−P bond length in the transition state.

to the *R*-configuration of the product.[17] This transition state was calculated to have the lowest energy, and the calculated results are given in Table 5. The addition to **10**-*syn*-below—transition state **TS-2** in Figure 4—is 9.2 kcal mol^{-1} higher in energy compared to **TS-1**. The much higher energy of **TS-2** compared to that of **TS-1** is also readable from the C−P distances in the transition states, as **TS-2** is a late transition state in which the C−P distance is 0.52 Å shorter compared to that in **TS-1**. The

(15) Frisch, M. J.; Trucks, G. W.; Schlegel, H. B.; Scuseria, G. E.; Robb, M. A.; Cheeseman, J. R.; Montgomery, J. A., Jr.; Vreven, T.; Kudin, K. N.; Burant, J. C.; Millam, J. M.; Iyengar, S. S.; Tomasi, J.; Barone, V.; Mennucci, B.; Cossi, M.; Scalmani, G.; Rega, N.; Petersson, G. A.; Nakatsuji, H.; Hada, M.; Ehara, M.; Toyota, K.; Fukuda, R.; Hasegawa, J.; Ishida, M.; Nakajima, T.; Honda, Y.; Kitao, O.; Nakai, H.; Klene, M.; Li, X.; Knox, J. E.; Hratchian, H. P.; Cross, J. B.; Bakken, V.; Adamo, C.; Jaramillo, J.; Gomperts, R.; Stratmann, R. E.; Yazyev, O.; Austin, A. J.; Cammi, R.; Pomelli, C.; Ochterski, J. W.; Ayala, P. Y.; Morokuma, K.; Voth, G. A.; Salvador, P.; Dannenberg, J. J.; Zakrzewski, V. G.; Dapprich, S.; Daniels, A. D.; Strain, M. C.; Farkas, O.; Malick, D. K.; Rabuck, A. D.; Raghavachari, K.; Foresman, J. B.; Ortiz, J. V.; Cui, Q.; Baboul, A. G.; Clifford, S.; Cioslowski, J.; Stefanov, B. B.; Liu, G.; Liashenko, A.; Piskorz, P.; Komaromi, I.; Martin, R. L.; Fox, D. J.; Keith, T.; Al-Laham, M. A.; Peng, C. Y.; Nanayakkara, A.; Challacombe, M.; Gill, P. M. W.; Johnson, B.; Chen, W.; Wong, M. W.; Gonzalez, C.; Pople, J. A. *Gaussian 03*, revision C.02; Gaussian, Inc.: Wallingford, CT, 2004.

(16) For DFT calculation of the approach of heteroaromatic compounds to the iminium ion intermediate, see: Dinér, P.; Nielsen, M.; Marigo, M.; Jørgensen, K. A. *Angew. Chem., Int. Ed.* **2007**, *46*, 1983.

(17) Please observe that the assignment of the absolute configuration changes for the alkyl-substituted compounds compared to **9h** in Figure 2.

SCHEME 4. Mechanistic Details of the Stereoselectivity in the Reaction Course

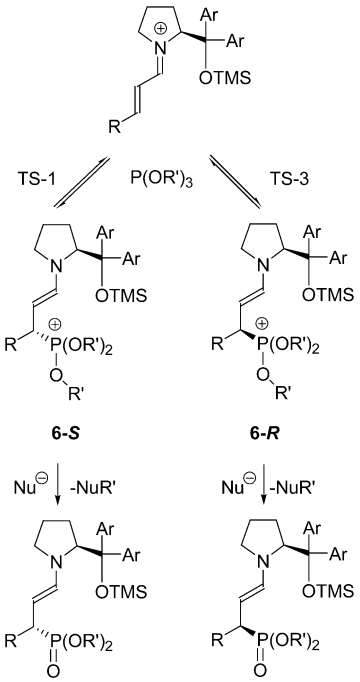

transition state for addition of **2a** to the shielded face (**10**-*anti*-upper in Figure 3) (**TS-3**) of the (*E*)-iminium ion leading to the *S*-configuration of the product, shown in Figure 4, is disfavored by 2.5 kcal mol^{-1}, compared to **TS-1**. This energy difference predicts the formation of the experimentally formed enantiomer. The calculated C−P distances in the transition states **TS-1** and **TS-3** are very similar, 2.34 and 2.39 Å, for the lowest and highest energy transition states, respectively.

In Scheme 4 is outlined what we propose to be the two most important steps in the catalytic cycle in Figure 1, in relation to formation of the two diastereomeric intermediates and the dealkylation steps that follow, leading to the two enantiomers of the product. The calculations of the transition states show that **TS-1**, to the left in Scheme 4, has the lowest energy leading to the kinetically favored intermediate. Furthermore, this intermediate **6**-*S* is also the most stable, due to less steric repulsion between the 2-substituent in the catalyst and the phosphonium fragment. Thus, a much higher concentration of intermediate **6**-*S*, compared to **6**-*R*, is present at this stage of the reaction. However, due to a higher energy of intermediate **6**-*R*, it might be expected that the dealkylation step of this intermediate proceeds faster than for **6**-*S*. The enantiomeric excess of the product in the β-phosphonylation reaction thus depends on both the concentration of the diastereomers **6**-*S* and **6**-*R* and the rate of the dealkylation of these two intermediates. For nucleophiles having a high *n* parameter, a fast dealkylation reaction takes place, leading to the high enantiomeric excess when NaI is used (see Table 3). For a poor nucleophile, the equilibrium between the diastereomeric intermediates **6**-*S* and **6**-*R* might change toward the latter, due to the higher reactivity of this intermediate. This will affect the equilibrium between **6**-*S* and **6**-*R*, and by a retro-Michael reaction, the concentration of **6**-*S* will be lower, resulting in a lower enantiomeric excess of the reaction.

Application and Synthesis. The optically active β-phosphonate aldehydes **3**, formed by the direct β-phosphonylation of the α,β-unsaturated aldehydes, are versatile intermediates for a number of important molecules. In the following, we will outline the synthesis of a number of these molecules.

SCHEME 5. Reduction of the Aldehyde Phosphonates and Esterification of the Corresponding Alcohols

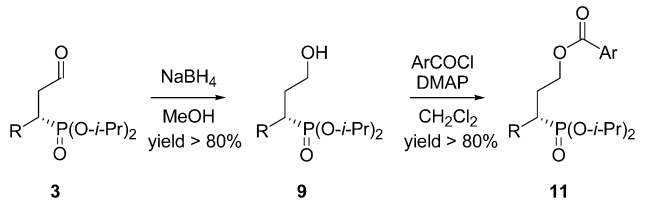

SCHEME 6. Preparation of the Phosphonic Acid Derivatives

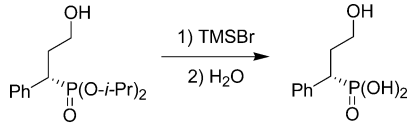

SCHEME 7. Glutamic Acid Precursor Synthesis via a Strecker Reaction

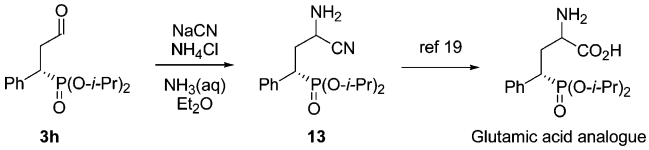

We were pleased to find that phosphonates **3** undergo a reduction to the corresponding alcohols **9** without any racemization, and the alcohols formed can be easily esterified to give **11** in good yields (Scheme 5). This procedure was used for the determination of the enantiomeric excesses in Table 4.

After initial reduction of the aldehyde to the alcohol (such as **9h**), the corresponding phosphonic acids can be prepared in good yields without any racemization using trimethysilylbromide for 36 h, followed by hydrolysis with H_2O (Scheme 6).[7c]

We next chose to focus our attention on the synthesis of glutamic acid analogues. The glutamic acid (Glu) receptor field has been and continues to be in a state of major development, as the number of known applications of Glu neurotransmitter system in chronic and acute diseases and disease conditions increases.[6b] Moreover, when the distal carboxylic acid of Glu is replaced with an acidic bioisosteres group, such as a phosphonic acid function, the selectivity of the receptor is enhanced.[5b]

Starting from the aldehyde **3h**, the glutamic acid precursor **13** can be formed in one step using the Strecker reaction.[18] The reaction of **3h** with sodium cyanide and ammonium chloride in a mixture of aq ammonia and Et_2O leads to the cyanoamine phosphonate **13** in 75% yield in a 1:1 diastereomeric ratio (Scheme 7).

Finally, the oxo-phosphonate **3** can also constitute an important intermediate in the fosmidomycin derivative synthesis (Scheme 8). Recently, several groups described an interest in derivatives of fosmidomycin and FR9000098 and their biological activities in anti-malarial studies.[7c,d] The compound **14c**,

(18) (a) Marvel, C. S.; Noyes, W. A. *J. Am. Chem. Soc.* **1920**, *42*, 2259. For a review on enantioselective Strecker reactions, see: (b) Gröger, H. *Chem. Rev.* **2003**, *103*, 2795. (c) Williams, R. M.; Hendrix, J. A. *Chem. Rev.* **1992**, *92*, 889.

(19) Varlet, J. M.; Fabre, G.; Sauveur, F.; Collignon, N.; Savignae, P. *Tetrahedron* **1981**, *37*, 1377.

SCHEME 8. Access to Fosmidomycin Derivatives

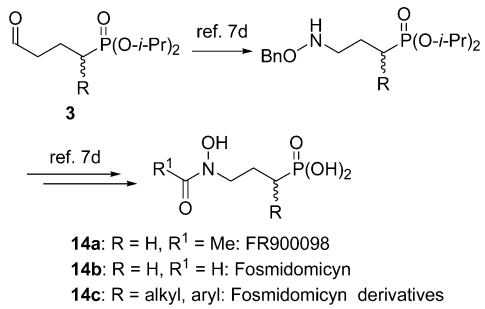

substituted in the α-position to the phosphonate moiety, has been found to be even more efficient than **14a**,**b**, whereas it was tested as a racemate.

Our new organocatalytic approach can be used to access a whole new family of fosmidomycin derivatives in a enantiopure manner, by switching the starting α,*β*-unsaturated aldehyde, which should lead to improved anti-malarial activities.

Conclusion

In summary, we have developed a new and simple direct asymmetric phosphonylation of α,*β*-unsaturated aldehydes. The key step of the phosphite addition is, besides the enantioselective step, the P(III)−P(V) transformation, which occurs via a nucleophilic S_N2-type dealkylation made possible by the use of NaI in combination with a Brønsted acid. The catalytic reaction affords the phosphonates in good yields and enantioselectivities for a broad range of enals, including aliphatic, aromatic, and heteroaromatic α,*β*-unsaturated aldehydes. Furthermore, we have demonstrated that the process is a convenient access to various important biologically active phosphonates and phosphonate derivatives, such as fosmidomycin or glutamic acid precursors. DFT calculations of the transition states predict the observed enantioselection of the phosphonylation reaction.

Experimental Section

General Procedure for the Phosphite Addition to α,*β*-Unsaturated Aldehydes. In an ordinary vial, the corresponding phosphite **2** (0.3 mmol) and NaI (0.3 mmol) were added to a stirred solution of catalyst **4a** (0.03 mmol), $PhCO_2H$ (0.6 mmol), and α,*β*-unsaturated aldehyde **1** (0.9 mmol) in CH_2Cl_2 (3 mL) at rt. After complete consumption of the phosphite (as monitored by ^{31}P NMR spectroscopy), the crude was directly charged in FC (eluent: Et_2O/MeOH 98/2) affording the pure products.

Experimental Data of Aldehydes. Diisopropyl [(1*R*)-1-(2-oxoethyl)butyl]phosphonate (**3c**). Yellow oil. Yield: 61% using catalyst (*S*)-**4a** and CH_2Cl_2 as the solvent. The ee was determined after esterification of the corresponding alcohol; see **10c**: $[\alpha]_D = -11.5$ (*c* 0.5, CH_2Cl_2), 84% ee; ^1H NMR ($CDCl_3$) δ 9.76 (br s, 1H), 4.71 (m, 2H), 2.78 (m, 1H), 2.52 (m, 1H), 2.34 (m, 1H), 1.74 (m, 2H), 1.40 (m, 2H), 1.30 (m, 12H), 0.90 (t, $J = 7.2$ Hz, 3H); ^{13}C NMR ($CDCl_3$) δ 200.6 (d, $J = 11.2$ Hz), 70.3 (m), 43.0 (d, $J = 3.1$ Hz), 31.0 (d, $J = 143.1$ Hz), 31.1 (d, $J = 3.9$ Hz), 24.0 (d, $J = 5.4$ Hz), 20.8 (d, $J = 11.2$ Hz), 13.9; ^{31}P NMR ($CDCl_3$) δ 29.2 (s); HRMS calcd for $C_{12}H_{25}O_4PNa$ $[M + Na]^+$ 287.1388, found 287.1381.

Diisopropyl [(1*S*)-1-(2-oxoethyl)butyl]phosphonate (*ent*-**3c**). Yellow oil. Yield: 55% using catalyst (*R*)-**4a** and CH_2Cl_2 as the solvent. The ee was determined after esterification of the corresponding alcohol; see *ent*-**10c**: $[\alpha]_D = +11.3$ (*c* 0.5, CH_2Cl_2), 82% ee; ^1H NMR ($CDCl_3$) δ 9.76 (br s, 1H), 4.71 (m, 2H), 2.78 (m, 1H), 2.52 (m, 1H), 2.34 (m, 1H), 1.74 (m, 2H), 1.40 (m, 2H), 1.30 (m, 12H), 0.90 (t, $J = 7.2$ Hz, 3H); ^{13}C NMR ($CDCl_3$) δ 200.6 (d, $J = 11.2$ Hz), 70.3 (m), 43.0 (d, $J = 3.1$ Hz), 31.0 (d, $J = 143.1$ Hz), 31.1 (d, $J = 3.9$ Hz), 24.0 (d, $J = 5.4$ Hz), 20.8 (d, $J = 11.2$ Hz), 13.9; ^{31}P NMR ($CDCl_3$) δ 29.2 (s); HRMS calcd for $C_{12}H_{25}O_4PNa$ $[M + Na]^+$ 287.1388, found 287.1381.

Diisopropyl [(1*R*)-1-ethyl-3-oxopropyl]phosphonate (**3e**). Yellow oil. Yield: 54% using catalyst (*S*)-**4a** and CH_2Cl_2 as the solvent. The ee was determined after esterification of the corresponding alcohol; see **10e**: $[\alpha]_D = -7.6$ (*c* 0.5, CH_2Cl_2), 85% ee; ^1H NMR ($CDCl_3$) δ 9.77 (br s, 1H), 4.70 (m, 2H), 2.76 (m, 1H), 2.52 (m, 1H), 2.26 (m, 1H), 1.84 (m, 1H), 1.43 (m, 1H), 1.29 (m, 12H), 0.98 (t, $J = 7.6$ Hz, 3H); ^{13}C NMR ($CDCl_3$) δ 200.4 (d, $J = 11.4$ Hz), 70.3 (m), 42.6 (d, $J = 2.6$ Hz), 32.7 (d, $J = 143.6$ Hz), 24.1 (m), 22.1 (d, $J = 3.7$ Hz), 12.2 (d, $J = 11.0$ Hz); ^{31}P NMR ($CDCl_3$) δ 30.0 (s); HRMS calcd for $C_{11}H_{23}O_4PNa$ $[M + Na]^+$ 273.1232, found 273.1234.

Diisopropyl [(1*R*,3*E*)-1-(2-oxoethyl)hept-3-en-1-yl]phosphonate (**3f**). Yellow oil. Yield: 46% using catalyst (*S*)-**4a** and CH_2Cl_2 as the solvent. The ee was determined after esterification of the corresponding alcohol; see **10f**: $[\alpha]^{23}_D = -5.3$ (*c* 0.5, CH_2Cl_2), 84% ee; ^1H NMR ($CDCl_3$) δ 9.76 (br s, 1H), 5.39 (m, 1H), 5.28 (m, 1H), 4.70 (m, 2H), 2.79 (m, 1H), 2.52 (m, 1H), 2.36 (m, 1H), 2.13 (q, $J = 8.0$ Hz, 2H), 2.02 (quint, $J = 7.2$ Hz, 2H), 1.82 (m, 1H), 1.46 (m, 1H), 1.30 (m, 12H), 0.95 (t, $J = 7.6$ Hz, 3H); ^{13}C NMR ($CDCl_3$) δ 200.2 (d, $J = 10.5$ Hz), 132.9 (d, $J = 2.2$ Hz), 127.5 (d, $J = 3.9$ Hz), 70.4 (m), 42.9 (d, $J = 2.9$ Hz), 30.8 (d, $J = 71.6$ Hz), 28.9 (d, $J = 3.8$ Hz), 25.1 (d, $J = 10.2$ Hz), 24.0 (d, $J = 4.2$ Hz), 20.5, 14.3; ^{31}P NMR ($CDCl_3$) δ 31.1 (s); HRMS calcd for $C_{15}H_{29}O_4PNa$ $[M + Na]^+$ 327.1701, found 327.1706.

Diisopropyl [(1*R*)-3-(*tert*-butyldimethylsilanyloxy)-1-(2-oxoethyl)propyl] phosphonate (**3g**). Yellow oil. Yield: 41% using catalyst (*S*)-**4a** and CH_2Cl_2 as the solvent. The ee was determined after esterification of the corresponding alcohol **10g**: $[\alpha]_D = -5.2$ (*c* 0.5, CH_2Cl_2), 82% ee; ^1H NMR ($CDCl_3$) δ 9.74 (br s, 1H), 4.73 (m, 2H), 3.69 (m, 2H), 2.77 (m, 1H), 2.59 (m, 2H), 2.04 (m, 1H), 1.60 (m, 1H), 1.30 (m, 12H), 0.88 (s, 9H), 0.03 (s, 6H); ^{13}C NMR ($CDCl_3$) δ 200.5 (d, $J = 11.6$ Hz), 70.4 (m), 60.5 (d, $J = 12.3$ Hz), 42.7 (d, $J = 3$ Hz), 31.7 (d, $J = 3.3$ Hz), 28.2 (d, $J = 144.7$ Hz), 25.9, 24.0, 18.2, −5.4; ^{31}P NMR ($CDCl_3$) δ 29.7 (s); HRMS calcd for $C_{17}H_{37}O_5PSiNa$ $[M + Na]^+$ 403.2046, found 403.2041.

Diisopropyl [(1*S*)-3-oxo-1-phenylpropyl]phosphonate (**3h**). Colorless oil. Yield: 51% using catalyst (*S*)-**4a** and CH_2Cl_2 as the solvent. The ee was determined after reduction to the corresponding alcohol **9h**: $[\alpha]_D = -1.2$ (*c* 0.07, CH_2Cl_2), 83% ee; ^1H NMR ($CDCl_3$) δ 9.68 (br s, 1H), 7.42−7.22 (m, 5H), 4.66 (m, 1H), 4.42 (m, 1H), 3.66 (ddd, $J = 23.2$, 8.8, 6.0 Hz, 1H), 3.14 (m, 2H), 1.29 (t, $J = 7.2$ Hz, 6H), 1.24 (d, $J = 6.4$ Hz, 3H), 0.91 (d, $J = 6.4$ Hz, 3H); ^{13}C NMR ($CDCl_3$) δ 199.3 (d, $J = 16.1$ Hz), 136.4 (d, $J = 6.7$ Hz), 129.2 (d, $J = 6.5$ Hz), 128.5 (d, $J = 2.4$ Hz), 127.4 (d, $J = 3.1$ Hz), 71.6 (d, $J = 7.2$ Hz), 70.7 (m), 44.2, 38.7 (d, $J = 142.5$ Hz), 30.3, 24.2 (m), 23.9 (m), 23.2 (m); ^{31}P NMR ($CDCl_3$) δ 25.3 (s); HRMS calcd for $C_{15}H_{23}O_4PNa$ $[M + Na]^+$ 321.1232, found 321.1227.

Diisopropyl [(1*S*)-1-(4-methoyphenyl)-3-oxopropyl]phosphonate (**3i**). Colorless oil. Yield: 67% using catalyst (*S*)-**4a** and CH_2Cl_2 as the solvent. The ee was determined after reduction to the corresponding alcohol **9i**: $[\alpha]_D = -0.7$ (*c* 0.5, CH_2Cl_2), 88% ee; ^1H NMR ($CDCl_3$) δ 9.67 (s, 1H), 7.31 (d, $J = 8.4$ Hz, 2H), 6.87 (d, $J = 8.4$ Hz, 2H), 4.70−4.62 (m, 1H), 4.47−4.40 (m, 1H), 3.80 (s, 3H), 3.61 (ddd, $J = 22.4$, 9.2, 5.6 Hz, 1H), 3.13−3.07 (m, 2H), 1.30 (t, $J = 6.8$ Hz, 6H), 1.25 (d, $J = 6.4$ Hz, 3H), 0.97 (d, $J = 6.4$ Hz, 3H); ^{13}C NMR ($CDCl_3$) δ 199.5 (d, $J = 16.0$ Hz), 158.8, 130.3 (d, $J = 7.0$ Hz), 127.1 (d, $J = 7.0$ Hz), 113.9, 71.6 (d, $J = 7.1$ Hz), 70.6 (m), 55.2, 44.3, 37.7 (d, $J = 142.9$ Hz), 24.2, 23.9, 23.2 (m); ^{31}P NMR ($CDCl_3$) δ 25.7 (s); HRMS calcd for $C_{16}H_{25}O_5PNa$ $[M + Na]^+$ 351.1337, found 351.1315.

Diisopropyl {(1*S*)-1-[4-(dimethylamino)phenyl]-3-oxopropyl}-phosphonate (**3j**). Yellow oil. Yield: 55% using catalyst (*S*)-**4a** and CH_2Cl_2 as the solvent. The ee was determined after reduction to the corresponding alcohol **9j**: $[\alpha]_D = +2.6$ (*c* 0.07, CH_2Cl_2),

74% ee; ^{1}H NMR ($CDCl_3$) δ 9.64 (br s, 1H), 7.21 (dd, J = 8.8, 2.0 Hz, 2H), 6.66 (d, J = 8.4 Hz, 2H), 4.62 (m, 1H), 4.40 (m, 1H), 3.52 (m, 1H), 3.04 (m, 2H), 2.91 (s, 6H), 1.26 (m, 9H), 0.95 (d, J = 6.0 Hz, 3H); ^{13}C NMR ($CDCl_3$) δ 200.0 (d, J = 15.2 Hz), 149.8, 129.9, 129.8, 112.6, 71.4 (d, J = 7.4 Hz), 70.4 (m), 44.5, 40.5, 37.7 (d, J = 142.4 Hz), 24.2, 24.0, 23.4 (m); ^{31}P NMR ($CDCl_3$) δ 25.1 (s); HRMS calcd for $C_{17}H_{28}NO_4PNa$ [M + Na]$^+$ 364.1654, found 364.1657.

Diisopropyl [(1*S*)-1-(4-chlorophenyl)-3-oxopropyl]phosphonate (**3k**). Colorless oil. Yield: 56% using catalyst (*S*)-**4a** and CH_2Cl_2 as the solvent. The ee was determined after reduction to the corresponding alcohol **9k**: $[\alpha]_D = -2.0$ (*c* 0.5, CH_2Cl_2), 88% ee; ^{1}H NMR ($CDCl_3$) δ 9.61 (s, 1H), 7.27−7.22 (m, 4H), 4.64−4.54 (m, 1H), 4.44−4.36 (m, 1H), 3.57 (ddd, J = 23.2, 9.6, 4.8 Hz, 1H), 3.14−2.98 (m, 2H), 1.28−1.18 (m, 6H), 0.92 (d, J = 6.0 Hz, 3H); ^{13}C NMR ($CDCl_3$) δ 198.7 (d, J = 15.9 Hz), 134.1 (d, J = 7.6 Hz), 133.2, 130.5, 128.6, 71.6 (d, J = 6.9 Hz), 70.8 (m), 44.2, 37.9 (d, J = 141.9 Hz), 24.1, 23.9, 23.3 (m); ^{31}P NMR ($CDCl_3$) δ 25.2 (s); HRMS calcd for $C_{15}H_{22}ClO_4PNa$ [M + Na]$^+$ 355.0842, found 355.0816.

Diisopropyl [(1*S*)-1-(2-furyl)-3-oxopropyl]phosphonate (**3l**). Yellow oil. Yield: 60% using catalyst (*S*)-**4a** and CH_2Cl_2 as the solvent. The ee was determined after esterification of the corresponding alcohol **9l**: $[\alpha]_D = -6.9$ (*c* 0.5, CH_2Cl_2), 74% ee; ^{1}H NMR ($CDCl_3$) δ 9.71 (t, J = 1.2 Hz, 1H), 7.33 (m, 1H), 6.32 (m, 1H), 6.27 (m, 1H), 4.6 (m, 2H), 3.85 (m, 1H), 3.07 (m, 1H), 1.25 (m, 9H), 1.16 (d, J = 6.0 Hz, 3H); ^{13}C NMR ($CDCl_3$) δ 198.9 (d, J = 14.9 Hz), 148.8, 141.9 (t, J = 2.9 Hz), 110.8 (m), 108.2 (m), 71.6 (m), 42.2 (d, J = 2.1 Hz), 32.8 (d, J = 146.2 Hz), 23.7 (m); ^{31}P NMR ($CDCl_3$) δ 21.5 (s); HRMS calcd for $C_{13}H_{21}O_5PNa$ [M + Na]$^+$ 311.1024, found 311.1018.

Diisopropyl [(1*S*)-3-oxo-1-(2-thienyl)propyl]phosphonate (**3m**). Yellow oil. Yield: 50% using catalyst (*S*)-**4a** and CH_2Cl_2 as the solvent. The ee was determined after reduction to the corresponding alcohol **9m**: $[\alpha]_D = -5.8$ (*c* 0.6, CH_2Cl_2), 84% ee; ^{1}H NMR ($CDCl_3$) δ 9.69 (s, 1H), 7.19−7.18 (m, 1H), 7.04−7.02 (m, 1H), 6.95−6.92 (m, 1H), 4.69−4.50 (m, 2H), 3.96 (ddd, J = 22.8, 9.6, 4.8 Hz, 1H), 3.17−3.01 (m, 2H), 1.29−1.25 (m, 9H), 1.06 (d, J = 6.4 Hz, 3H); ^{13}C NMR ($CDCl_3$) δ 198.9 (d, J = 15.0 Hz), 137.4, 127.0, 126.9, 124.8, 72.0 (m), 71.2 (m), 45.2, 33.9 (d, J = 152.1 Hz), 24.1 (m), 23.9 (m), 23.3 (m); ^{31}P NMR ($CDCl_3$) δ 24.4 (s); HRMS calcd for $C_{13}H_{21}O_4PSNa$ [M + Na]$^+$ 327.0796, found 327.0764.

General Procedure for the Reduction of Aldehydes. The aldehyde is dissolved in MeOH, and then 2 equiv of $NaBH_4$ is added. After 2 h, the solution is quenched with distilled H_2O before being extracted with CH_2Cl_2. The organic phase is dried over $MgSO_4$, evaporated, and purified by FC using Iatrobeads (eluent: Et_2O/MeOH 98/2) affording the pure product.

Experimental Data of Alcohols. Diisopropyl [(1*S*)-3-hydroxy-1-phenylpropyl]phosphonate (**9h**). White solid. The ee was determined by HPLC using a Daicel Chiralcel OD column [hexane/*i*PrOH 90:10]; flow rate = 1.0 mL/min; τ_{minor} = 8.7 min, τ_{major} = 10.0 min (83% ee); $[\alpha]^{20}_D = +9.4$ (*c* 1.0, CH_2Cl_2); ^{1}H NMR ($CDCl_3$) δ 7.35−7.23 (m, 5H), 4.65 (m, 1H), 4.44 (m, 1H), 3.68 (m, 1H), 3.47 (m, 1H), 3.18 (ddd, J = 22.4, 9.6, 5.2 Hz, 1H), 2.45 (br s, 1H), 2.30 (m, 1H), 2.13 (m, 1H), 1.27 (t, J = 6.4 Hz, 6H), 1.21 (d, J = 6.0 Hz, 3H), 0.92 (d, J = 6.0 Hz, 3H); ^{13}C NMR ($CDCl_3$) δ 136.4 (d, J = 6.6 Hz), 129.3 (d, J = 6.9 Hz), 128.4 (d, J = 2.0 Hz), 127.0 (d, J = 2.8 Hz), 71.2 (d, J = 7.6 Hz), 70.3 (m), 60.2 (m), 42.6 (d, J = 0.8 Hz), 41.9 (d, J = 139.1 Hz), 33.6 (d, J = 2.6 Hz), 25.3, 24.2, 24.0 (m), 23.2 (m); ^{31}P NMR ($CDCl_3$) δ 26.9 (s); HRMS calcd for $C_{15}H_{25}O_4PNa$ [M + Na]$^+$ 323.1388, found 323.1393.

Diisopropyl [(1*S*)-3-hydroxy-1-(4-methoxyphenyl)propyl]phosphonate (**9i**). Colorless oil. The ee was determined by HPLC using a Daicel Chiralcel OJ column [hexane/*i*PrOH 97:3]; flow rate = 1.0 mL/min; τ_{minor} = 42.4 min, τ_{major} = 48.3 min (88% ee); $[\alpha]^{20}_D = +12.3$ (*c* 0.7, CH_2Cl_2); ^{1}H NMR ($CDCl_3$) δ 7.26−7.23 (m, 2H), 6.84 (d, J = 8.8 Hz, 2H), 4.69−4.61 (m, 1H), 4.48−4.40 (m, 1H), 3.78 (s, 3H), 3.70−3.65 (m, 1H), 3.50−3.44 (m, 1H), 3.13 (ddd, J = 22.4, 9.6, 5.2 Hz, 1H), 2.35−2.20 (m, 2H), 2.15−2.03 (m, 1H), 1.29−1.21 (m, 9H), 0.96 (d, J = 6.4 Hz, 3H); ^{13}C NMR ($CDCl_3$) δ 158.6 (d, J = 3.0 Hz), 130.3 (d, J = 7.0 Hz), 128.2 (d, J = 7.0 Hz), 113.8, 71.1 (d, J = 7.5 Hz), 70.2 (m), 60.3 (d, J = 13.3 Hz), 55.2 (m), 41.0 (d, J = 140.1 Hz), 33.6, 24.2, 23.9, 23.3 (m); ^{31}P NMR ($CDCl_3$) δ 27.8 (s); HRMS calcd for $C_{16}H_{27}O_5PNa$ [M + Na]$^+$ 353.1497, found 353.1148.

Diisopropyl {(1*S*)-1-[4-(dimethylamino)phenyl]-3-hydroxypropyl}-phosphonate (**9j**). White solid. The ee was determined by HPLC using a Daicel Chiralcel OD column [hexane/*i*PrOH 90:10]; flow rate = 1.0 mL/min; τ_{major} = 13.0 min, τ_{minor} = 16.1 min (74% ee); $[\alpha]^{20}_D = +3.0$ (*c* 1.0, CH_2Cl_2); ^{1}H NMR ($CDCl_3$) δ 7.18 (d, J = 8.4 Hz, 2H), 6.67 (d, J = 8.4 Hz, 2H), 4.66 (m, 1H), 4.44 (m, 1H), 3.68 (m, 1H), 3.48 (m, 1H), 3.18 (ddd, J = 22.8, 9.6, 5.2 Hz, 1H), 2.92 (s, 6H), 2.30 (m, 2H), 2.10 (m, 1H), 1.27 (t, J = 6.4 Hz, 6H), 1.22 (d, J = 6.4 Hz, 3H), 0.97 (d, J = 6.4 Hz, 3H); ^{13}C NMR ($CDCl_3$) δ 149.6 (s), 129.9 (d, J = 7.0 Hz), 123.7 (m), 112.6 (s), 71.0 (d, J = 7.2 Hz), 70.1 (m), 60.3 (d, J = 13.6 Hz), 40.8 (d, J = 140.1 Hz), 40.6 (s), 33.6 (s), 24.2 (d, J = 2.6 Hz), 24.0 (d, J = 4.2 Hz), 23.4 (d, J = 5.6 Hz); ^{31}P NMR ($CDCl_3$) δ 28.6 (s); HRMS calcd for $C_{15}H_{25}O_4PNa$ [M + Na]$^+$ 366.1810, found 366.1813.

Diisopropyl [(1*S*)-1-(4-chlorophenyl)-3-hydroxypropyl]phosphonate (**9k**). Yellow solid. The ee was determined by HPLC using a Daicel Chiralpak AD column [hexane/*i*PrOH 90:10]; flow rate = 1.0 mL/min; τ_{major} = 13.2 min, τ_{minor} = 24.4 min (88% ee); $[\alpha]^{20}_D = -6.8$ (*c* 0.5, CH_2Cl_2); ^{1}H NMR ($CDCl_3$) δ 7.20−7.19 (m, 4H), 4.69−4.56 (m, 1H), 4.46−4.38 (m, 1H), 3.65−3.60 (m, 1H), 3.44−3.35 (m, 1H), 3.13 (ddd, J = 22.4, 10.0, 5.2 Hz, 1H), 2.29−2.27 (m, 1H), 2.19−1.95 (m, 1H), 1.22−1.16 (m, 9H), 0.94 (d, J = 6.0 Hz, 3H); ^{13}C NMR ($CDCl_3$) δ 135.1 (d, J = 7.0 Hz), 132.9, 130.6 (d, J = 7.0 Hz), 128.6, 71.2 (d, J = 7.1 Hz), 70.6 (m), 60.0 (d, J = 12.8 Hz), 41.3 (d, J = 139.9 Hz), 33.4, 24.1 (m), 23.9, 23.4 (m); ^{31}P NMR ($CDCl_3$) δ 27.2 (s); HRMS calcd for $C_{15}H_{24}ClO_4PNa$ [M + Na]$^+$ 357.0998, found 357.1002.

Diisopropyl [(1*S*)-3-hydroxy-1-(2-thienyl)propyl]phosphonate (**9m**). Yellow solid. The ee was determined by HPLC using a Daicel Chiralcel OD column [hexane/iPrOH 95:5]; flow rate = 1.0 mL/min; τ_{minor} = 16.2 min, τ_{major} = 19.7 min (84% ee); $[\alpha]^{20}_D = +3.9$ (*c* 0.5, CH_2Cl_2); ^{1}H NMR ($CDCl_3$) δ 7.19 (d, J = 5.2 Hz, 1H), 7.03−7.01 (m, 1H), 6.96 (d, J = 4.8 Hz, 1H), 4.73−4.53 (m, 2H), 3.78−3.73 (m, 1H), 3.58−3.48 (m, 2H), 2.35−2.07 (m, 3H), 1.31−1.26 (m, 9H), 1.08 (d, J = 6.0 Hz, 3H); ^{13}C NMR ($CDCl_3$) δ 138.4, 126.8, 124.4, 71.6, 70.8, 60.0 (d, J = 12.8 Hz), 37.1 (d, J = 144.4 Hz), 34.9, 24.2, 23.9, 23.4; ^{31}P NMR ($CDCl_3$) δ 25.4 (s); HRMS calcd for $C_{13}H_{21}O_4PSNa$ [M + Na]$^+$ 329.0952, found 329.0958.

General Procedure for the Esterification. The crude obtained after reduction of the aldehyde is dissolved in CH_2Cl_2, and 2.2 equiv of 4-nitrobenzoyl chloride is added, followed by a catalytic amount of DMAP and 2.2 equiv of Et_3N, and the mixture is stirred for 4 h. Then, the solution is successively washed with a 1 M HCl solution and a saturated $NaHCO_3$ solution, dried with $MgSO_4$, and the solvent is evaporated. The crude is purified by FC using Iatrobeads (eluent: Et_2O/MeOH 98/2) affording the pure product.

Experimental Data of Esters. (3*R*)-3-(Diisopropoxyphosphoryl)hexyl 4-nitrobenzoate (**11c**). Colorless oil. The ee was determined by HPLC using a Daicel Chiralcel OD column [hexane/*i*PrOH 95:5]; flow rate = 1.0 mL/min; τ_{minor} = 13.0 min, τ_{major} = 14.0 min; $[\alpha]^{23}_D = -10.6$ (*c* 0.5, CH_2Cl_2, 84% ee); ^{1}H NMR ($CDCl_3$) δ 8.28 (d, J = 8.0 Hz, 2H), 8.19 (d, J = 8.4 Hz, 2H), 4.72 (m, 2H), 4.50 (t, J = 6.8 Hz, 2H), 2.17 (m, 1H), 1.96 (m, 1H), 1.80 (m, 2H), 1.46 (m, 3H), 1.30 (m, 12H), 0.91 (t, J = 6.8 Hz, 3H); ^{13}C NMR ($CDCl_3$) δ 164.5, 150.5, 135.6, 130.6 (m), 123.5, 70.0 (d, J = 5.7 Hz), 64.2 (d, J = 8.5 Hz), 33.6 (d, J = 141.5 Hz), 30.6 (d, J = 3.9 Hz), 27.5 (d, J = 2.8 Hz), 24.1 (m), 20.7 (d, J = 10.9 Hz), 14.0; ^{31}P NMR ($CDCl_3$) δ 30.0 (s); HRMS calcd for $C_{19}H_{30}NO_7PNa$ [M + Na]$^+$ 438.1658, found 438.1675.

(3*S*)-3-(Diisopropoxyphosphoryl)hexyl 4-nitrobenzoate (*ent*-**11c**). Colorless oil. The ee was determined by HPLC using a Daicel Chiralcel OD column [hexane/*i*PrOH 95:5]; flow rate = 1.0 mL/min; τ_{major} = 12.2 min, τ_{minor} = 14.0 min; $[\alpha]^{23}_D = +10.4$ (*c* 0.5, CH_2Cl_2, 82% ee); ^{1}H NMR ($CDCl_3$) δ 8.28 (d, J = 8.0 Hz, 2H), 8.19 (d, J = 8.4 Hz, 2H), 4.72 (m, 2H), 4.50 (t, J = 6.8 Hz, 2H), 2.17 (m, 1H), 1.96 (m, 1H), 1.80 (m, 2H), 1.46 (m, 3H), 1.30 (m, 12H), 0.91 (t, J = 6.8 Hz, 3H); ^{13}C NMR ($CDCl_3$) δ 164.5, 150.5, 135.6, 130.6 (m), 123.5, 70.0 (d, J = 5.7 Hz), 64.2 (d, J = 8.5 Hz), 33.6 (d, J = 141.5 Hz), 30.6 (d, J = 3.9 Hz), 27.5 (d, J = 2.8 Hz), 24.1 (m), 20.7 (d, J = 10.9 Hz), 14.0; ^{31}P NMR ($CDCl_3$) δ 30.0 (s).

(3*R*)-3-(Diisopropoxyphosphoryl)pentyl 4-nitrobenzoate (**11e**). Colorless oil. The ee was determined by HPLC using a Daicel Chiralcel OD column [hexane/*i*PrOH 97:3]; flow rate = 1.0 mL/min; τ_{minor} = 21.4 min, τ_{major} = 22.8 min; $[\alpha]^{23}_D = -11.6$ (*c* 0.5, CH_2Cl_2, 85% ee); ^{1}H NMR ($CDCl_3$) δ 8.29 d, J = 9.2 Hz, 2H), 8.20 (d, J = 9.2 Hz, 2H), 4.72 (m, 2H), 4.49 (t, J = 6.8 Hz, 2H), 2.19 (m, 1H), 1.98 (m, 1H), 1.81 (m, 2H), 1.57 (m, 1H), 1.31 (m, 12H), 1.05 (t, J = 7.2 Hz, 3H); ^{13}C NMR ($CDCl_3$) δ 164.5, 150.5, 135.6, 130.6, 123.5, 70.0 (m), 64.2 (d, J = 8.9 Hz), 35.3 (d, J = 141.2 Hz), 27.0 (d, J = 2.9 Hz), 24.1 (m), 21.5 (d, J = 3.7 Hz), 12.2 (d, J = 10.3 Hz); ^{31}P NMR ($CDCl_3$) δ 30.5 (s); HRMS calcd for $C_{18}H_{28}NO_7PNa$ $[M + Na]^+$ 424.1501, found 424.1501.

(3*R*,5*Z*)-3-(Diisopropoxyphosphoryl)non-5-en-1-yl 4-nitrobenzoate (**11f**). Colorless oil. The ee was determined by HPLC using a Daicel Chiralcel OD column [hexane/*i*PrOH 98:2]; flow rate = 1.0 mL/min; τ_{minor} = 21.9 min, τ_{major} = 24.4 min; $[\alpha]^{23}_D = -2.0$ (*c* 0.5, CH_2Cl_2, 84% ee); ^{1}H NMR ($CDCl_3$) δ 8.28 (d, J = 7.2 Hz, 2H), 8.20 (d, J = 7.2 Hz, 2H), 5.40 (m, 1H), 5.29 (m, 1H), 4.73 (m, 2H), 4.50 (t, J = 6.8 Hz, 2H), 2.20 (m, 3H), 2.03 (m, 3H), 1.85 (m 2H), 1.50 (m, 1H), 1.31 (m, 12H), 0.93 (t, J = 7.2 Hz, 3H); ^{13}C NMR ($CDCl_3$) δ 164.5, 150.4, 135.6, 132.9 (m), 130.7, 127.6 (m), 123.5, 70.1 (m), 64.1 (d, J = 8.3 Hz), 36.2 (d, J = 141.7 Hz), 28.5 (d, J = 13.6 Hz), 27.5 (d, J = 12.8 Hz), 25.0 (d, J = 39.2 Hz), 24.1, 20.6, 14.3; ^{31}P NMR ($CDCl_3$) δ 30.5 (s); HRMS calcd for $C_{22}H_{34}NO_7PNa$ $[M + Na]^+$ 478.1971, found 478.1961.

(3*R*)-5-(*tert*-Butyldimethylsilanyloxy)-3-(diisopropoxyphosphoryl)pentyl 4-nitro benzoate (**11g**). Colorless oil. The ee was determined by HPLC using a Daicel Chiralcel OD column [hexane/*i*PrOH 97:3]; flow rate = 1.0 mL/min; τ_{minor} = 13.2 min, τ_{major} = 14.8 min; $[\alpha]^{23}_D = -10.8$ (*c* 0.5, CH_2Cl_2, 82% ee); ^{1}H NMR ($CDCl_3$) δ 8.28 (d, J = 8.4 Hz, 2H), 8.19 (d, J = 8.4 Hz, 2H), 4.72 (m, 2H), 4.51 (t, J = 6.8 Hz, 2H), 3.75 (t, J = 6.0 Hz, 1H), 2.20 (m, 1H), 2.03 (m, 3H), 1.67 (m, 1H), 1.32 (m, 12H), 0.85 (s, 9H), 0.03 (s, 6H); ^{13}C NMR ($CDCl_3$) δ 164.5, 150.4, 135.7, 130.7, 123.5, 70.2 (m), 64.2 (d, J = 9.4 Hz), 60.5 (d, J = 10.3 Hz), 31.7 (d, J = 2.7 Hz), 30.2 (d, J = 142.0 Hz), 27.7, 25.7, 24.1 (d, J = 3.0 Hz), 18.2, −5.4; ^{31}P NMR ($CDCl_3$) δ 30.3 (s); HRMS calcd for $C_{24}H_{42}NO_8PSiNa$ $[M + Na]^+$ 554.2315, found 554.2318.

(3*S*)-3-(Diisopropoxyphosphoryl)-3-(2-furyl)propyl 4-nitrobenzoate (**11l**). Yellow oil. The ee was determined by HPLC using a Daicel Chiralpak AD column [hexane/*i*PrOH 90:10]; flow rate = 1.0 mL/min; τ_{major} = 23.6 min, τ_{minor} = 27.2 min; $[\alpha]^{23}_D = +30.2$ (*c* 0.5, CH_2Cl_2, 74% ee); ^{1}H NMR ($CDCl_3$) δ 8.27 (d, J = 7.6 Hz, 2H), 8.13 (d, J = 7.6 Hz, 2H), 7.34 (m, 1H), 6.33 (m, 1H), 6.31 (m, 1H), 4.67 (m, 2H), 4.58 (m, 1H), 4.42 (m, 1H), 4.26 (m, 1H), 3.38 (m, 1H), 2.50 (m, 1H), 2.39 (m, 1H), 1.29 (m, 9H), 1.11 (d, J = 6.4 Hz, 3H); ^{13}C NMR ($CDCl_3$) δ 164.4, 150.5, 149.2 (d, J = 8.7 Hz), 142.0, 135.4, 130.7, 123.5, 110.9 (m), 108.4 (m), 71.3 (m), 63.8 (d, J = 15.7 Hz), 36.1 (d, J = 148.0 Hz), 28.7 (d, J = 1.8 Hz), 24.0 (m), 23.6; ^{31}P NMR ($CDCl_3$) δ 21.8 (s); HRMS calcd for $C_{20}H_{26}NO_8PNa$ $[M + Na]^+$ 462.1294, found 462.1300.

Reductive Amination of Aldehyde 3a. To a solution of aldehyde **3a** in dichloroethane were added aniline (1 equiv), $NaBH(OAc)_3$ (1.5 equiv), and AcOH (1 equiv) at rt, and the resulting mixture was stirred for 4 h. Then, the solution was successively washed with a 1 M NaOH aq solution and brine, and the organic layer was dried over $MgSO_4$, and the solvent was evaporated. The pure compound was obtained after FC purification (eluent: Et_2O/MeOH 98/2). Colorless oil. The ee was determined by HPLC using a Daicel Chiralpak AD column [hexane/*i*PrOH 98:2]; flow rate = 1.0 mL/min; τ_{major} = 25.6 min, τ_{minor} = 28.3 min; $[\alpha]^{23}_D = -10.3$ (*c* 0.5, CH_2Cl_2, 59% ee); ^{1}H NMR ($CDCl_3$) δ 7.19−7.15 (m, 2H), 6.68 (t, J = 6.8 Hz, 1H), 6.61 (d, J = 8.0 Hz, 2H), 3.76 (s, 3H), 3.73 (s, 3H), 3.27−3.23 (m, 2H), 2.02−1.69 (m, 4H), 1.51−1.37 (m, 4H), 0.91 (t, J = 6.8 Hz, 3H); ^{13}C NMR ($CDCl_3$) δ 148.0, 129.2, 117.2, 112.7, 52.4 (m), 41.9 (d, J = 7.7 Hz), 33.2 (d, J = 131.2 Hz), 30.7, 28.1, 20.8, 20.7, 14.0; ^{31}P NMR ($CDCl_3$) δ 37.2 (s); HRMS calcd for $C_{14}H_{24}NO_3PNa$ $[M + Na]^+$ 308.1391, found 308.1402.

Procedure for the Phosphonic Acids Synthesis. The alcohol **9h** was mixed with 10 equiv of bromotrimethylsilane for 36 h. The excess of bromotrimethylsilane was then evaporated, and the mixture was hydrolyzed with distilled H_2O for 5 h. H_2O was then evaporated and the crude dried under high vacuum conditions, affording the desired product **12** in 80% yield. Colorless oil. The ee was determined by realkylation of **11** (see below) (82% ee); $[\alpha]^{20}_D = +44.4$ (*c* 1.0, MeOH); ^{1}H NMR (D_2O) δ 7.45−7.30 (m, 5H), 3.52 (br s, 1H), 3.35 (br s, 1H), 3.18−3.28 (q, 1H), 2.25 (br s, 1H), 2.15 (br s, 1H); ^{13}C NMR (D_2O) δ 136.1 (d, J = 7.4 Hz), 129.2 (d, J = 6.4 Hz), 128.6 (d, J = 2.5 Hz), 127.4 (d, J = 3.2 Hz), 59.2 (d, J = 16.9 Hz), 41.4 (d, J = 132.8 Hz), 31.4 (d, J = 2.5 Hz); ^{31}P NMR (D_2O) δ 27.9 (s); HRMS calcd for $C_9H_{13}O_4PNa$ $[M + Na]^+$ 239.0449, found 239.0446.

Procedure for the Methylation of the Phosphonic Acid. The phosphonic acid **12** (25 mg, 0.12 mmol) was dissolved in 0.2 mL of a mixture of MeOH and CH_2Cl_2 (5:1) under N_2. A 2.0 M solution of (trimethylsilyl)diazomethane in hexanes (0.35 mL, 0.70 mmol, 6 equiv) was added dropwise over 30 s. After 2 h, the reaction was concentrated in vacuo. The crude residue was purified by FC on Iatrobeads (Et_2O/MeOH 98/2) to provide the desired product **9h″** in 60% yield (18 mg, 0.07 mmol), which was directly used for ee determination by chiral HPLC. Colorless oil. The ee was determined by HPLC using a Daicel Chiralcel AD column [hexane/*i*PrOH 80:20]; flow rate = 1.0 mL/min; τ_{major} = 14.7 min, τ_{minor} = 15.5 min (82% ee); $[\alpha]^{20}_D = +15.4$ (*c* 1.0, CH_2Cl_2); ^{1}H NMR ($CDCl_3$) δ 7.38−7.22 (m, 5H), 3.69 (d, J = 11.6 Hz, 3H), 3.66 (br s, 1H), 3.51 (d, J = 10.4 Hz, 3H), 3.47 (br s, 1H), 3.32 (m, 1H), 2.32 (m, 1H), 2.17 (m, 1H); ^{13}C NMR ($CDCl_3$) δ 135.6 (s), 129.2 (d, J = 6.8 Hz), 128.6 (d, J = 2.2 Hz), 127.3 (d, J = 3.1 Hz), 59.9 (d, J = 13.5 Hz), 40.5 (d, J = 138.1 Hz), 33.4 (d, J = 2.9 Hz), 30.3; ^{31}P NMR ($CDCl_3$) δ 31.6 (s); HRMS calcd for $C_{11}H_{17}O_4PNa$ $[M + Na]^+$ 267.0762, found 267.0760.

Procedure for the Strecker Reaction. The aldehyde **3h** (60 mg, 0.2 mmol) is dissolved in a mixture of Et_2O (0.2 mL), and an aqueous solution of NH_3 (0.2 mL) then NH_4Cl (10.7 mg, 0.2 mmol, 1 equiv) and NaCN (9.8 mg, 0.2 mmol, 1 equiv) are successively added. The reaction is stirred for 30 h, and then the crude is directly charged by chromatography using Iatrobeads to afford the pure product **13** in 75% yield. Less polar diastereoisomer: colorless oil; $[\alpha]^{20}_D = +11.0$ (*c* 0.5, CH_2Cl_2); ^{1}H NMR ($CDCl_3$) δ 7.35−7.25 (m, 5H), 4.66 (m, 1H), 4.43 (m, 1H), 3.40 (br m, 1H + 1H), 2.38 (m, 2H), 1.67 (br d, 2H), 1.29 (m, 6H), 1.22 (d, J = 6.4 Hz, 3H) 0.82 (d, J = 6.4 Hz, 3H); ^{13}C NMR ($CDCl_3$) δ 134.6 (d, J = 6.7 Hz), 129.4 (d, J = 6.6 Hz), 128.7 (d, J = 2.2 Hz), 127.7 (d, J = 2.7 Hz), 122.0, 71.5 (d, J = 7.3 Hz), 70.5 (m), 40.9 (d, J = 141.4 Hz), 40.4 (d, J = 16.8 Hz), 35.9, 30.3, 24.2 (d, J = 3.0 Hz), 24.0 (m), 23.2 (d, J = 5.6 Hz); ^{31}P NMR ($CDCl_3$) δ 25.6 (s); HRMS calcd for $C_{16}H_{25}N_2O_3PNa$ $[M + Na]^+$ 347.1500, found 347.1500. More polar diastereoisomer: colorless oil; $[\alpha]^{20}_D = +32.3$ (*c* 2.0, CH_2Cl_2); ^{1}H NMR ($CDCl_3$) δ 7.40−7.25 (m, 5H), 4.68 (m, 1H), 4.38 (m, 1H), 3.42 (t, J = 8.0 Hz, 1H), 3.25 (m, 1H), 2.39 (m, 2H), 2.00 (br d, 2H), 1.30 (m, 6H), 1.21 (d, J = 6.4 Hz, 3H), 0.86 (d, J = 6.4 Hz, 3H); ^{13}C NMR ($CDCl_3$) δ 134.5 (d, J = 6.9 Hz), 129.2 (d, J = 6.7 Hz), 128.8 (d, J = 2.3 Hz), 127.8 (d, J = 3.0 Hz), 121.1, 71.6 (d, J = 7.3 Hz), 70.6 (m), 42.3 (d, J = 18.0 Hz), 42.1 (d, J = 141.1 Hz), 36.1, 30.3, 24.2 (d, J = 2.8 Hz), 23.9 (m), 23.1 (d, J = 5.3 Hz); ^{31}P NMR ($CDCl_3$) δ 25.7 (s).

Acknowledgment. This work was made possible by a grant from The Danish National Research Foundation and OChemSchool. S.C. thanks Ministerio de Educación y Ciencia of Spain for a postdoctoral fellowship. Thanks are expressed to Dr. Jacob Overgaard from the Department of Chemistry, Aarhus University, for performing the X-ray crystal structure analysis.

Supporting Information Available: General methods, characterization, NMR and HPLC spectra, X-ray data, and computational data. This material is free of charge via the Internet at http://pubs.acs.org.

JO7018587